Front. Phys. China, 2009, 4(2): 144–154
DOI 10.1007/s11467-009-0026-6

REVIEW ARTICLE

Preliminary frequency measurement of the electric quadrupole transition in a single laser-cooled $^{40}Ca^{+}$ ion

Bin GUO (郭彬)[1,2,3], **Hua GUAN** (管桦)[1,2], **Qu LIU** (刘曲)[1,2,3], **Yao HUANG** (黄垚)[1,2,3]
Wan-cheng QU (屈万成)[1,2,3], **Xue-ren HUANG** (黄学人)[1,2](✉), **Ke-lin GAO** (高克林)[1,2](✉)

[1] *State Key Laboratory of Magnetic Resonance and Atomic and Molecular Physics, Wuhan Institute of Physics and Mathematics, Chinese Academy of Sciences, Wuhan 430071, China*
[2] *Center for Cold Atom Physics, Chinese Academy of Sciences, Wuhan 430071, China*
[3] *Graduate School, Chinese Academy of Sciences, Beijing 100080, China*
E-mail: hxueren@wipm.ac.cn, klgao@wipm.ac.cn

Received February 13, 2009; accepted February 27, 2009

The trapping and laser cooling of $^{40}Ca^{+}$ ion on the way toward optical frequency standards have been developed. A single $^{40}Ca^{+}$ ion is trapped in the miniature Paul trap and laser cooled by two frequency-stabilized diode lasers. A commercial Ti:Sapphire laser system at 729 nm is referenced to a high-finesse cavity to meet the requirements of ultra narrow linewidth of the $4s^2S_{1/2}$–$3d^2D_{5/2}$ electric quadrupole transition. Its center frequency is preliminarily measured to be 411 042 129 686.1 (2.6) kHz. The attempt to finally lock the 729-nm laser system to atomic transition is made. Further work to improve the accuracy of measurement and the stabilization of system locking is in consideration and preparation.

Keywords ion trap, optical frequency standard, laser stabilization, laser cooling

PACS numbers 32.80.Pj, 43.58.Hp

Contents

1 Introduction

The technical realization of laser cooling for neutral atoms and ions, ultra narrow linewidth laser system, and the wide bandwidth femtosecond comb bring the effort to improve atom and molecular precision spectroscopy successfully. In particular, direct measurements of frequencies in optical region result in rapid progress on optical frequency standard. The appearance of optical frequency standard based on single laser-cooled ion and neutral atoms is a breakthrough in timekeeping domain [1]. The optical frequency standard based on trapped ion was proposed by Dehmelt, and the predicted uncertainly of 10^{-18} level was 4–5 order of magnitudes better than microwave frequency standards [2]. Therefore, the frequency standards based on cold atoms have been considered to be the most potential candidates for the new definition of second and also for tests of the fundamental constants in physics. They could have applications such as geodesy.

Along with the evolution of the ion trap technique, single-ion frequency standard research is underway at a number of laboratories worldwide, including those based on Hg^+ [3, 4], Yb^+ [5, 6], In^+ [7], Sr^+ [8], Al^+[9], Ca^+ [10], and Ba^+ [11]. The Hg^+ and Al^+ ion optical clocks as the best frequency standards nowadays have reached the uncertainty of 1.9×10^{-17} and 2.3×10^{-17}, respectively [12]. Measurements with the uncertainty in the order of 10^{-15} were reported with Sr^+ and Yb^+. On the other hand, precision frequency measurements and com-

parison of the Al^+ and Hg^+ clock transitions contribute to searching for the possible temporal variation of the fine-structure constant α of $\dot{\alpha}/\alpha = (-1.6 \pm 2.3) \times 10^{-17}$ /year [12].

The optical frequency standard on the $^{40}Ca^+$ was also proposed [13, 14]. The technological advantage is that all necessary laser systems could be generated by commercially available and easy-to-handle solid-state lasers, and the odd isotope of $^{43}Ca^+$ ion that could be used as an optical frequency standard is immune to the first-order Zeeman frequency shift. The $^{40}Ca^+$ is also popular in atomic physics and quantum information [15], and numerous researches on $^{40}Ca^+$ were accomplished both in theory and experiment; the absolute frequency of the $4s^2S_{1/2}$–$3d^2D_{5/2}$ transition was just measured at 10^{-14} on the Paul trap [10] and 10^{-15} on the liner Paul trap [16].

The trapping and laser cooling of $^{40}Ca^+$ ions that have been carried out in the Wuhan Institute of Physics and Mathematics, Chinese Academy of Sciences, are on the way toward optical frequency standard. This article briefly summarizes and reports the research progress recently.

2 Spectroscopy

2.1 Ion trap and laser systems

The ion trap used in the experiments for trapping single $^{40}Ca^+$ ion is a miniature Paul trap (Fig. 1) [17, 18]. The trap is made up of a 1.6-mm diameter ring and two endcap electrodes 1.4 mm apart, which are made of 0.5-mm radius stainless steel wire. Two electrodes perpendicular to each other are set in the ring plane to compensate the ion's excess micromotion. The miniature structure makes for confining a single ion in the Lamb–Dick regime to eliminate the first-order Doppler effect of the 729-nm clock transition; the nonstandard configuration compared with the classical Paul trap can decrease background noise in the laser experiment.

Fig. 1 Ion trap experimental setup.

An RF drive voltage of 400 V_{p-p} at frequency of 10 MHz is applied to the ring as the electric trapping field. The fluorescence detection during the laser cooling process is achieved by photomultiplier tube (PMT) and photocount electrical equipments, which are controlled by computer with Lab VIEW programs. The trap is enclosed in a chamber that is evacuated to a pressure of less than 10^{-10} Torr.

To realize Doppler cooling, the $4^2S_{1/2}$–$4^2P_{1/2}$ transition at 397 nm is chosen according to the level scheme of $^{40}Ca^+$(Fig. 2). Because of the ion at $4^2P_{1/2}$ level decaying with a probability of 6% to the metastable $3^2D_{3/2}$ level, a repumping laser at 866 nm is required. The laser at 397 and 866 nm are both the commercial Littrow-type extended-cavity diode laser (Toptica DL-100).

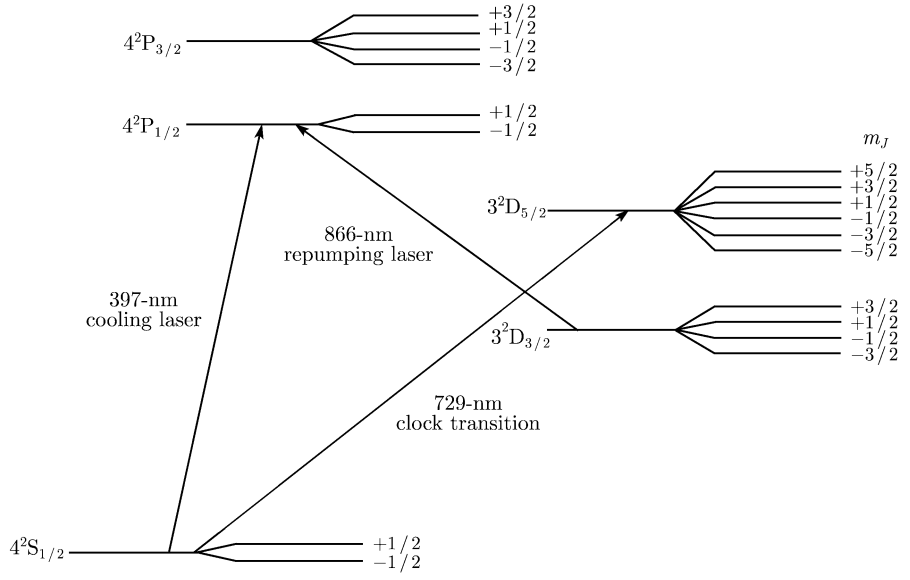

Fig. 2 Level scheme of $^{40}Ca^+$.

For the sake of optimizing the laser cooling effect, the linewidths of the cooling laser at 397 nm and repumping laser at 866 nm should be narrower than 1 MHz; also, the long drift should be controlled within 1 MHz per hour. The two diode lasers are frequency stabilized to the transmission peaks of commercial Fabry–Perot (F–P) cavities and further locked to the optogalvanic (OG) signal of calcium ions to improve the long-term drift performance. The linewidths (full width at half maximum (FWHM)) is 3–4 MHz, dithering about 2–3 MHz and with a long-term drift of 50 MHz in approximately 15 minutes (Fig. 3) [19].

For further decreasing of the linewidth and restraining the long-term drifts of the diode lasers, a transfer cavity is introduced into the cooling laser stabilization system [20, 21]. Using the ultra stable clock transition laser system at 729 nm as a reference, the laser at 397 nm is locked to the commercial F–P cavity, which is referenced to the clock transition laser by the home-made transfer cavity and computer programs (Fig. 4).

The repumping laser at 866 nm is stabilized in the same way as the 397-nm laser but without the prestable commercial F–P cavity. The error signal from the transfer cavity is directly fed back to the 866-nm ECDL's Piezo transformer (PZT), which controls the grating angle of diffraction.

Compared with about 50 MHz per hour of long drift before, the lasers at 397 and 866 nm are approximately optimized to 400 and 100 kHz per hour of long-term drift, respectively (Figs. 5, 6). Their linewidths are improved at the same time.

As to $^{40}Ca^{+}$ ion optical frequency standard, the $4s^2S_{1/2}$–$3d^2D_{5/2}$ electric quadrupole transition as clock transition has a natural linewidth of 0.16 Hz. So the probe laser at 729 nm need to reach the Hertz level stabilization. It is the sticking point in optical frequency standards.

The commercial Ti:sapphire laser used in 729-nm system is Coherent MBR-110, and its linewidth is worse than 50 kHz. The Pound–Drever–Hall (PDH) method is adopted to stabilize the 729-nm Ti:Sapphire laser with a super cavity (Fig. 7).

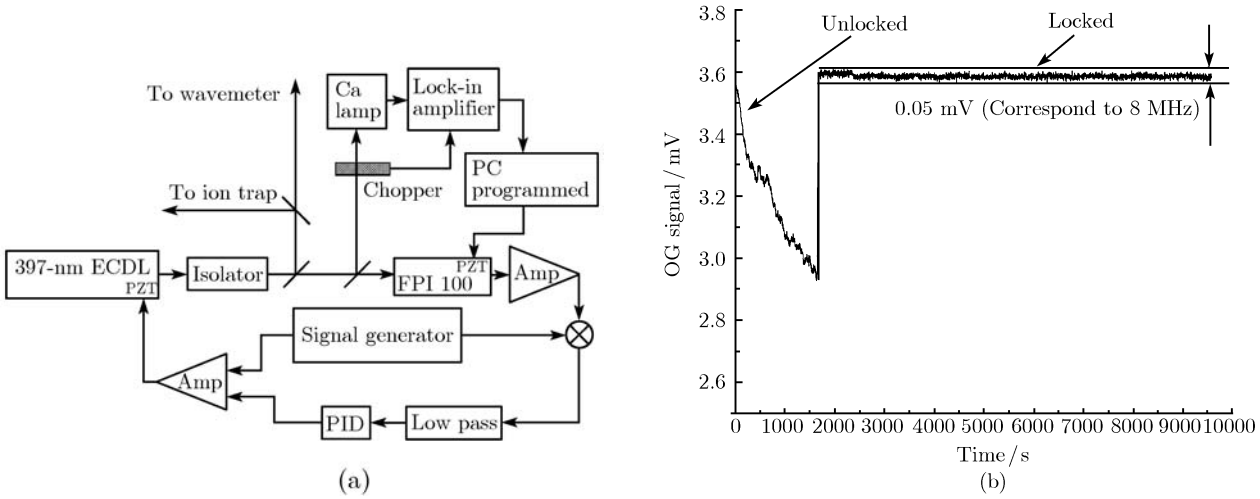

Fig. 3 **(a)** OG frequency stabilization scheme of the diode laser. The 397-nm laser is locked to a confocal F–P cavity, which is referenced to an OG signal of calcium ions; **(b)** OG signals before and after the cavity locking.

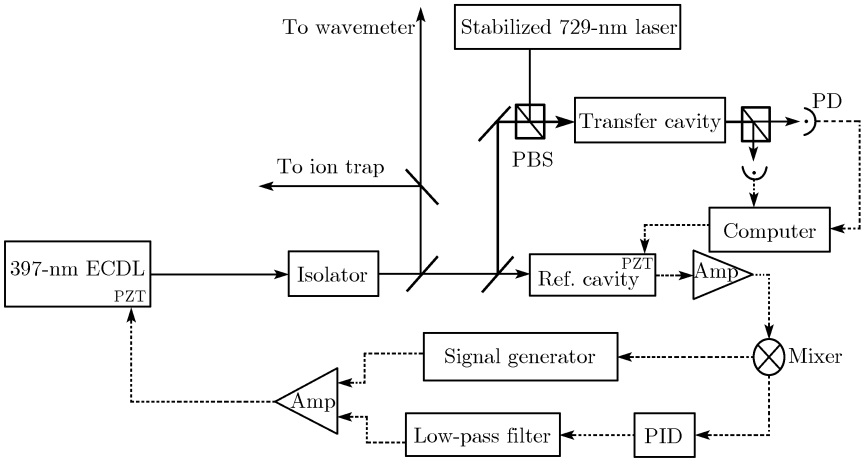

Fig. 4 Frequency stabilization scheme of the diode laser at 397 nm. ECDL: Extended cavity diode laser; Amp: Amplifier; PBS: Polarizing beam splitter; PD: Photo diode; Ref. cavity: Reference transfer cavity.

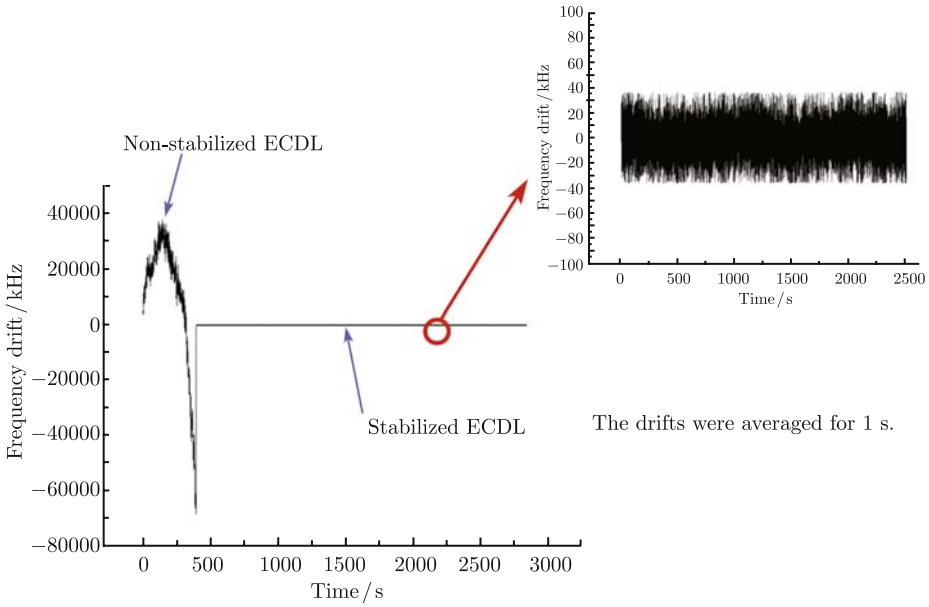

Fig. 5 Error signals before and after the transfer cavity locking of the 866-nm laser.

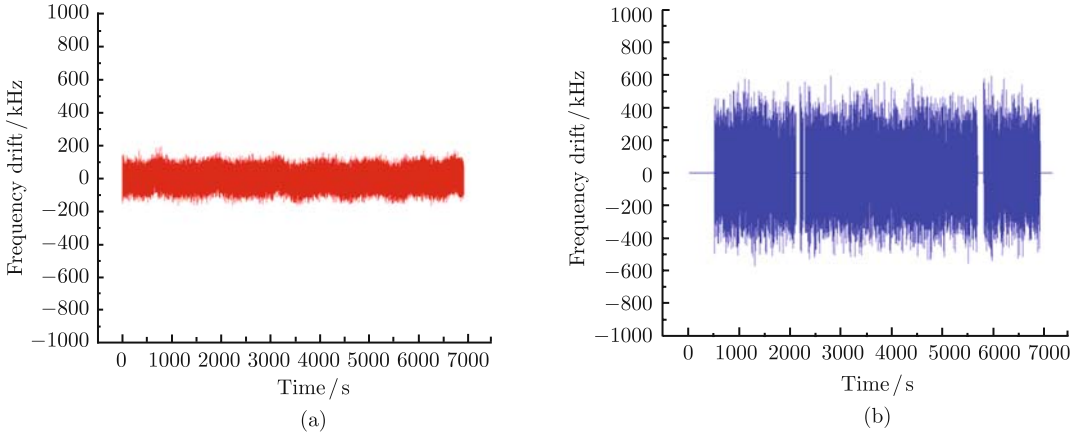

Fig. 6 Error signals of the lasers locked to the transfer cavities. **(a)** 397-nm laser; **(b)** 866-nm laser.

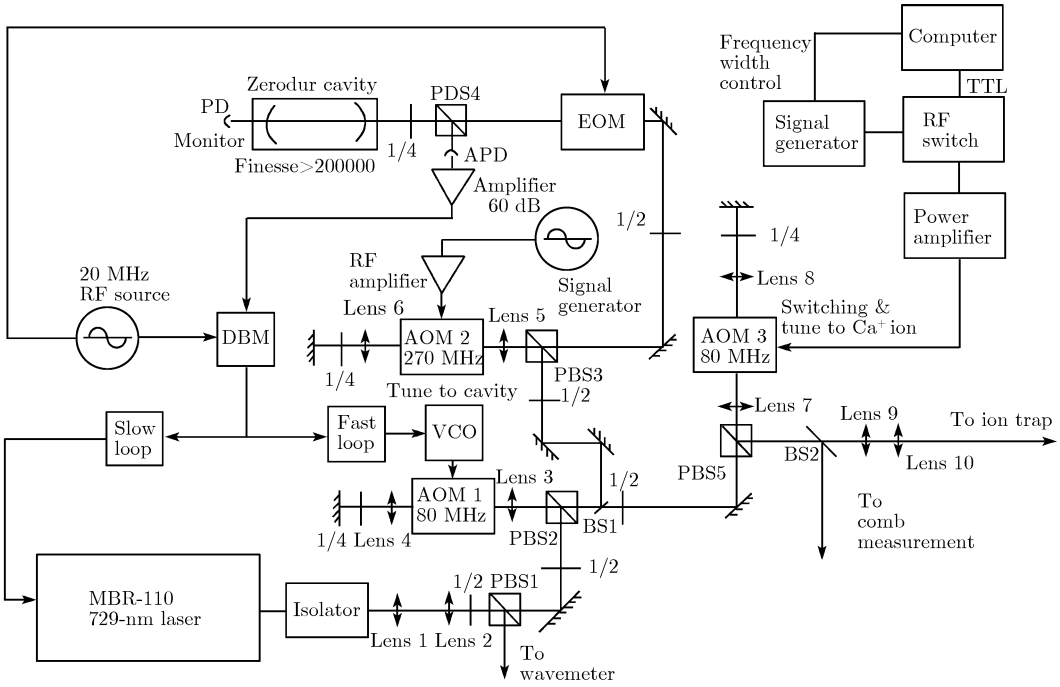

Fig. 7 Frequency stabilization scheme of the Ti:Sapphire laser at 729 nm.

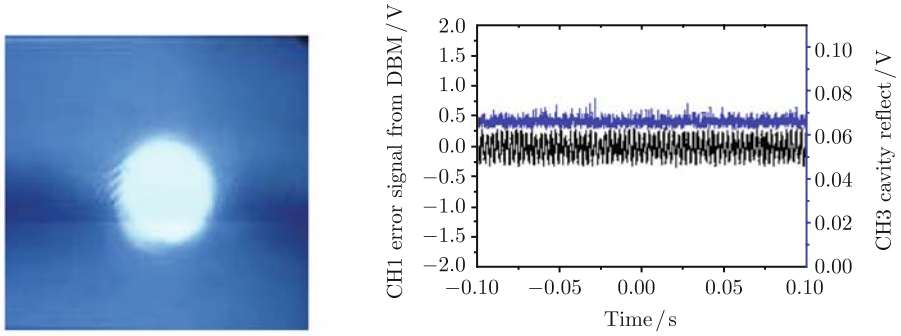

Fig. 8 The signal of MBR-110 stabilized to the super cavity. **(a)** The TEM_{00} mode; **(b)** The error signal (*black*) and the signal reflected by the cavity (*blue*).

The super cavity is made of Zerodur material with ultralow thermo-expanding coefficient. The spacer of the cavity is 200 mm long and 100 mm in diameter, enclosed in a chamber evacuated to 10^{-8} Torr. The finesse of the cavity is 350 000, measured by observing the intensity of the light field decaying out of the high-finesse cavity. The 729-nm laser's TEM $_{00}$ mode is coupled into the super cavity with an efficiency of 30%. The system was locked as the probe laser to drive the optical transition (Fig. 8).

Vibration isolation and double-layer temperature control are finished to improve system performance. Cavity's temperature drift is controlled within 10 mK. The resonance frequency drifts at the rate of 0.7 Hz per second in the best condition.

2.2 Spectroscopy

2.2.1 Ion trapping and micromotion compensation

First, the 397-nm laser frequency is red detuned about 600 MHz, and the 866-nm laser is set on the resonance. The $^{40}Ca^{+}$ ions are loaded by heating the atom oven through 3.5 A DC current to about 600°C, and 3 A DC current is applied on the filament for half a minute; the bias voltage of the filament is set to be –30 V. The Ca atoms are ionized in the trap center by the electron beam. The whole loading procedure lasts for about 2 minutes. Then, scanning cooling laser from red detuning to the resonance center, we can get the fluorescence spectrum. We can load a single $^{40}Ca^{+}$ ion at a probability of 50% of the trial. If more than one ion is loaded in the trap, we keep scanning the 397-nm laser from red detuning to blue detuning until we get one ion.

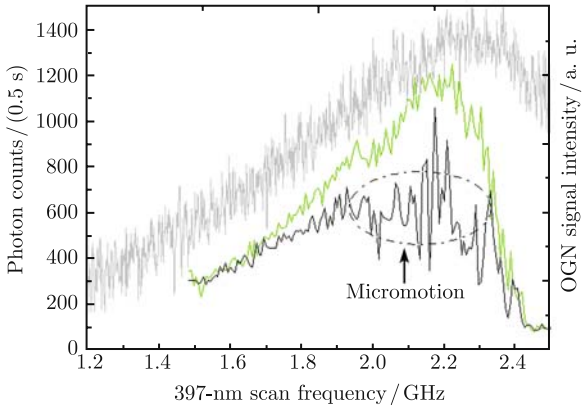

Fig. 9 Alterations of atomic transition line shape. The gray profile is the 397-nm laser OGN signal intensity.

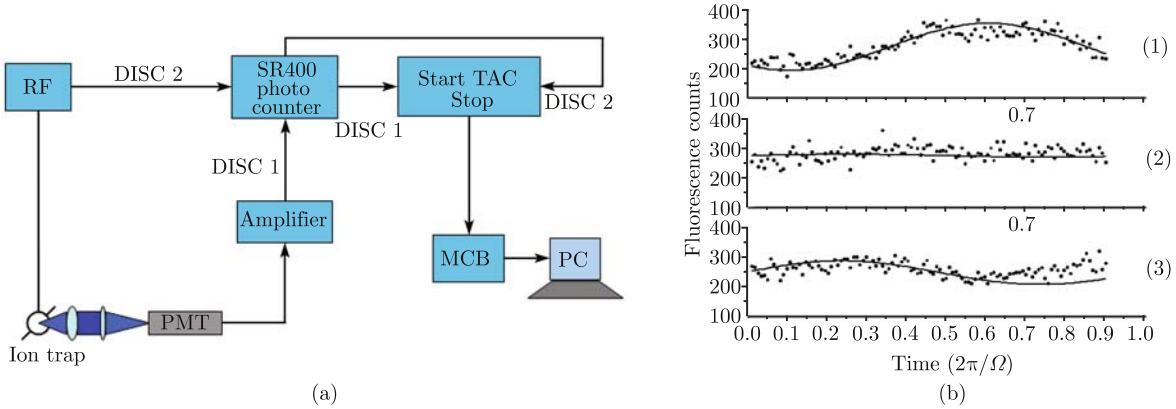

Fig. 10 **(a)** The photo-RF correlation experiment scheme. TAC: Time-to-Amplitude Converters, MCB: Multi-channel buffers. **(b)** The photo-RF correlation results with one of the endcap voltages different as $El = -5.444$, -4.999, and -4.512 V. The minimal micromotion in cooling laser direction is shown in the middle.

Except for stabilizing two cooling diode lasers, a single ion suffers the excess micromotion [22]. The amplitude of ion micromotion strongly depends on RF electric trapping field power and additional static electric field. Two methods of detecting ion micromotion are demonstrated. One relies on the alterations of atomic transition line shape (Fig. 9); the other depends on the photo-RF correlation technique (Fig. 10). The static voltages are added on the pair of endcaps, and compensation electrodes are adjusted slightly to minimize the excess micromotion.

The single ion fluorescence line shape and quantum jump signal are optimized by patients and repeated experiments step by step in recent years [17, 18]. The new results are better than ever before, a typical counting rate of 7000 s^{-1} was observed for the single cold $^{40}Ca^{+}$ ion (Fig. 11). Single ion can be trapped for more than 6 hours.

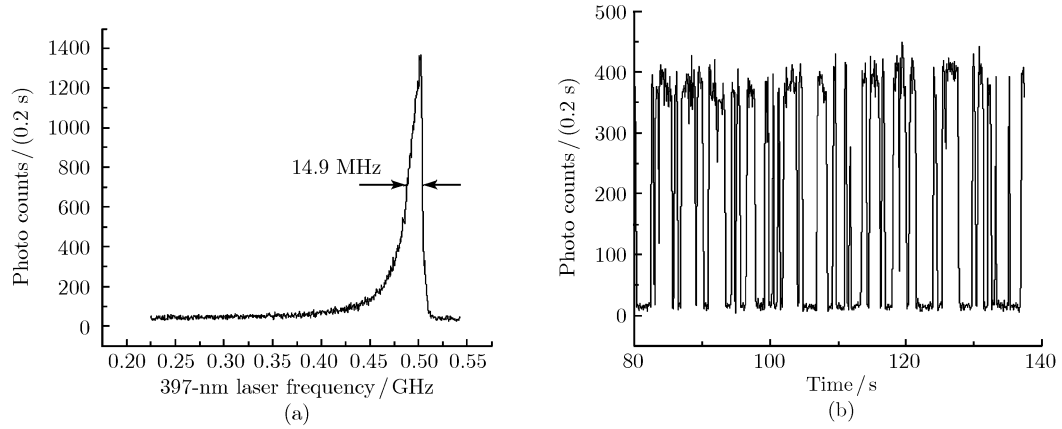

Fig. 11 **(a)** The line width of single ion fluorescence signal is about 14.9 MHz, and photo count rate is up to 7 kHz; **(b)** Single ion quantum jump signal with a signal-to-noise ratio better than 50 in 200 ms.

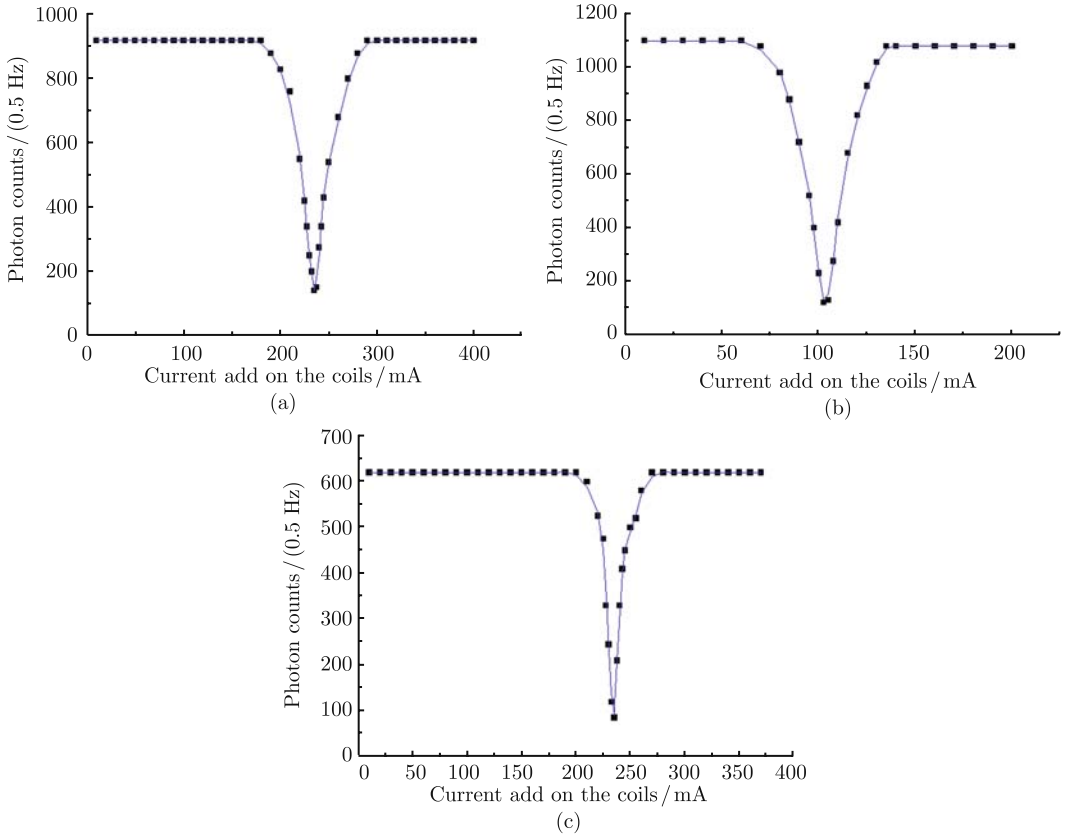

Fig. 12 The fluorescence signal vanishes when the magnetic fields that are perpendicular to the 866-nm laser's polarization direction are compensated to zero along three directions. The RF power supply is −400 V, 397 nm and 866 nm laser power into the trap is 30 μW and 200 μW respectively. **(a)** The magnetic field direction of vertical; **(b)** The magnetic field direction of laser beam; and **(c)** The magnetic field direction of PMT.

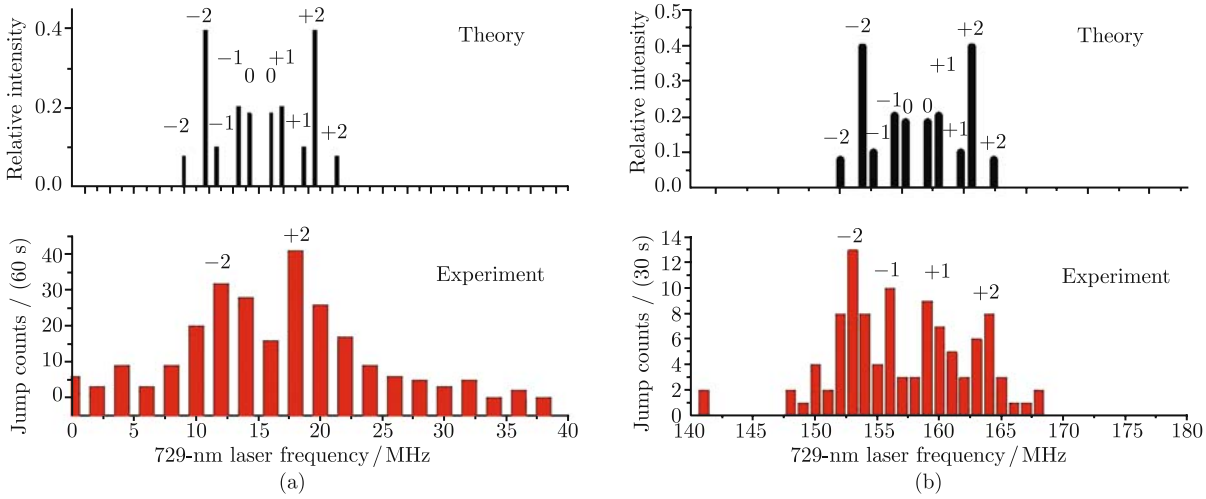

Fig. 13 The theory and experiment results of the single $^{40}Ca^{+}$ ion's $4s^2S_{1/2}$–$3d^2D_{5/2}$ optical clock transition Zeeman profile. **(a)** The scan step of the 729-nm laser is 2 MHz; the brief double peak structure of the profile is shown by the experiment result obviously. **(b)** The difference from **(a)** is the scan step of the 729-nm laser; the shorter scan step (1 MHz per step) shows the more elaborate profile structure.

2.2.2 Quadrupole transition measurement

The milestone to single $^{40}Ca^{+}$ ion optical frequency standard is the observation of the Zeeman components for the $4s^2S_{1/2}$–$3d^2D_{5/2}$ clock transition after accomplishing the ultra stable clock laser system. The magnetic field at the position of the ion trap center needs to be controlled well. The three magnet coil pairs aligned along three perpendicular directions (PMT, laser beam, and vertical) are set to generate an arbitrary magnetic field of up to 3 Gauss. The ambient magnetic field in the center of the trap is measured according to Hanle effect [23] (Fig. 12) (Table 1), which would give a Zeeman splitting of the 729-nm transition of about 12.35 MHz in theory for all 10 Zeeman components.

The quadrupole transition spectrum can be obtained by counting the number of the quantum jumps observed in a fixed period. The frequency region of clock transition should be found approximately in the ambient magnetic field with the 729-nm laser continuously running. The Zeeman profile is observed both in theory and experimentally (Fig. 13).

Table 1 The ambient magnetic field in the center of the trap.

Directions	Current add on the coils/mA	Ambient magnetic field /G
Laser beam	104±2	0.588±0.011
Vertical	−233±2	−1.137±0.010
PMT	235±2	0.920±0.008

The relative intensities of the components depend on the orientation of the polarization, the direction of propagation of the 729-nm laser, and the direction of the magnetic field [24]. When the 729-nm laser is chosen horizontal polarization along the direction of PMT, the perpendicular high magnetic field is generated by the vertical coil pair, and the transverse components are compensated by other coils; the clock transition only with $\Delta M_J = \pm 2$ can be driven selectively. Frequency distances between two pairs of components are only determined by the magnitude of the vertical magnetic field (Fig. 14). It should be clear that every peak is made up of corresponding Zeeman component and its secular motion sidebands approximately at 1 MHz, whose linewidths are strongly broadened because of the 397-nm cooling laser. The micromotion sidebands at 10 MHz, which is the RF trap frequency, are distinguished obviously.

The frequencies of the two peaks can be measured and taken to give the center frequency. To get the pure ten Zeeman components of the $4s^2S_{1/2}$–$3d^2D_{5/2}$ clock transition, we decrease the magnetic field so that the Zeeman splitting range shrinks, which separates the carrier from its nearest secular motion sideband. To reduce the profile linewidth, the cooling laser and clock laser must be chopped in antiphase pulse. The optical time sequence system is home made using the mechanical shutters, acousto-optic modulators (AOM), and the GPIB equipment (Fig. 15). The full Zeeman profile components of the clock transition are achieved successfully (Fig. 16).

2.2.3 Preliminary measurement of the clock transition and lock experiment

The two $\Delta M_J = 0$ components are considered to be a good reference to the atom optical frequency. The ultra narrow linewidth optical resonator can be stabilized in a

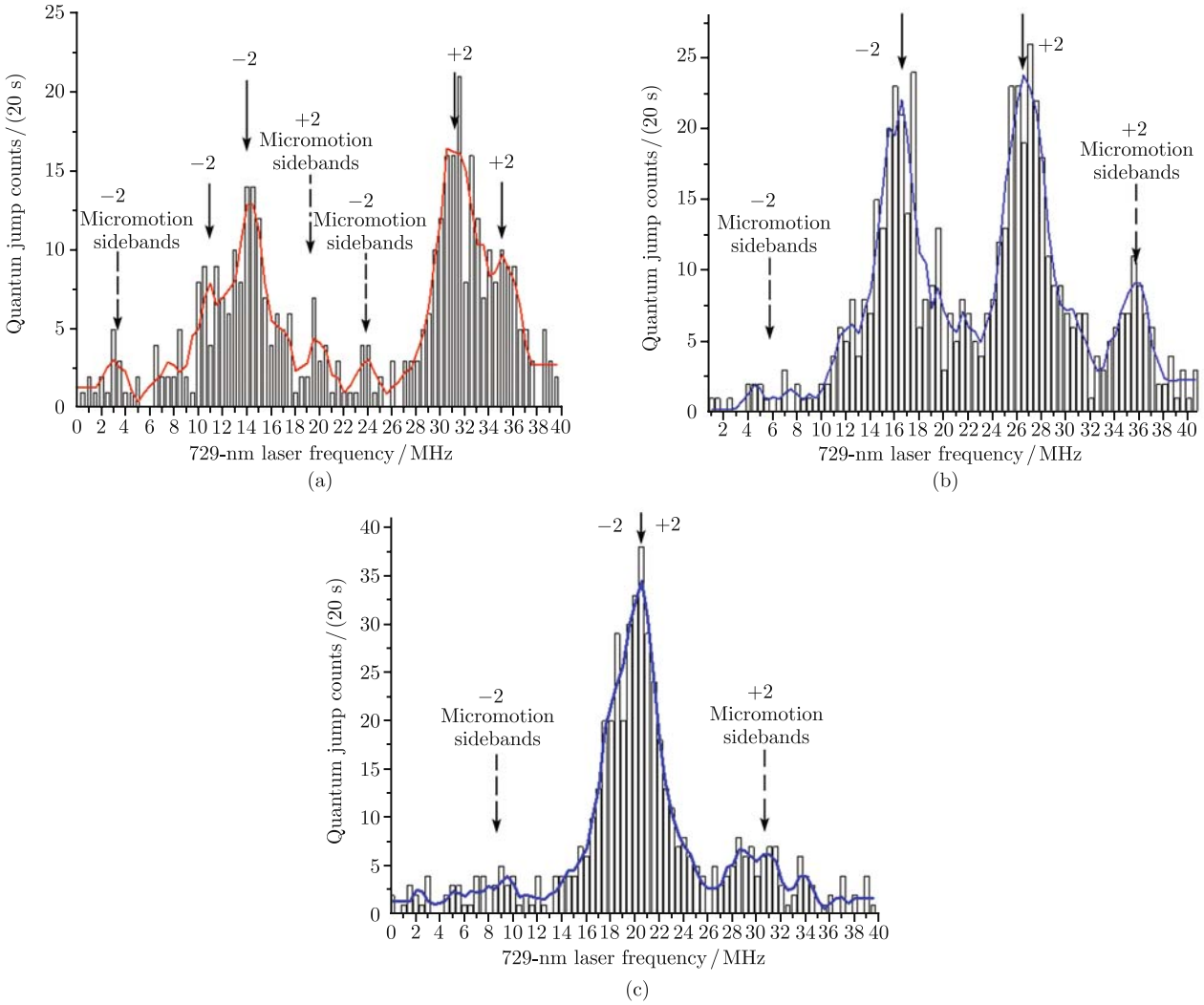

Fig. 14 The quantum jump profiles of the 729-nm transition in different ambient magnetic field. Two peaks of $\Delta M_J = \pm 2$ components of the transition close to each other, getting along with the reduction of vertical magnetic field. **(a)** 16.8 MHz distance between two components with high vertical magnetic field of 3.00 Gauss; **(b)** 10.0 MHz distance between two components with high vertical magnetic field of 1.79 Gauss; **(c)** Vertical magnetic field of 0.37 Gauss was applied and the unresolved Zeeman splitting over a total of 8-MHz linewidth. The solid profile is 7 points S–G smoothing to the bar profile.

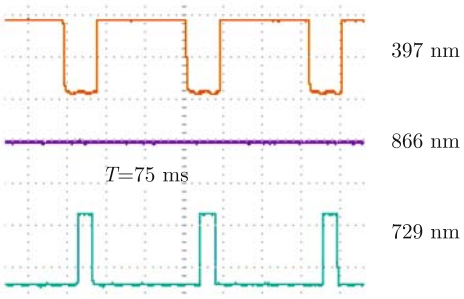

Fig. 15 The optical time sequence with the 729-nm pulse of 10 ms.

long term to that of two Zeeman components.

The linewidth of each Zeeman component is measured as 3–4 kHz, which still has large potential to be optimized (Fig. 17). To improve the result of the 729-nm clock transition frequency, the linewidth and the scan step width should be reduced as much as possible.

The center frequency of $^{40}Ca^{+}4s^2S_{1/2}$–$3d^2D_{5/2}$ optical clock transition could be measured by recording the results of 80 MHz AOM's quantum jump profiles of the two $\Delta M_J = 0$ Zeeman components and the super cavity's resonate frequency that is directly measured by a femtosecond comb system referenced to a standard RF 10-MHz signal from a hydrogen maser at the same time [25]. The output of the ULE-stabilized laser beam at 729 nm is divided into two parts. Major portion of the stabilized laser beam is fed into the frequency comb to measure the absolute optical frequency of the cavity; the other part is used to probe the $4s^2S_{1/2}$–$3d^2D_{5/2}$ clock transition modulated by a double-passed 80-MHz AOM. A frequency synthesizer (E4422B Agilent. Inc), which is also referenced to the 10-MHz RF signal from the hydrogen maser, is used to drive the AOM. The clock transition frequency f_{Ca} of $4s^2S_{1/2}$–$3d^2D_{5/2}$ can be given by

$$f_{Ca} = nf_{rep} \pm f_{ceo} \pm f_b + f_{AOM}$$

where f_{AOM} is the frequency of the frequency synthesizer output for AOM, which is used to tune the ULE cavity frequency to match the clock transition of $^{40}Ca^{+}$ ion.

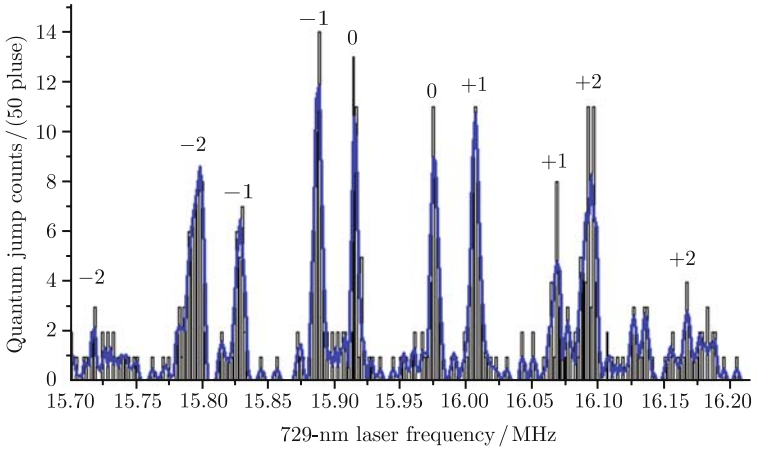

Fig. 16 Ten components of the Zeeman profile $4s^2S_{1/2}$–$3d^2D_{5/2}$ clock transition with the whole separation of 432 kHz in the magnetic field of 55 milli-Guass is scanned by the optical time pulse. The solid profile is 5 points S–G smoothing to bar profile.

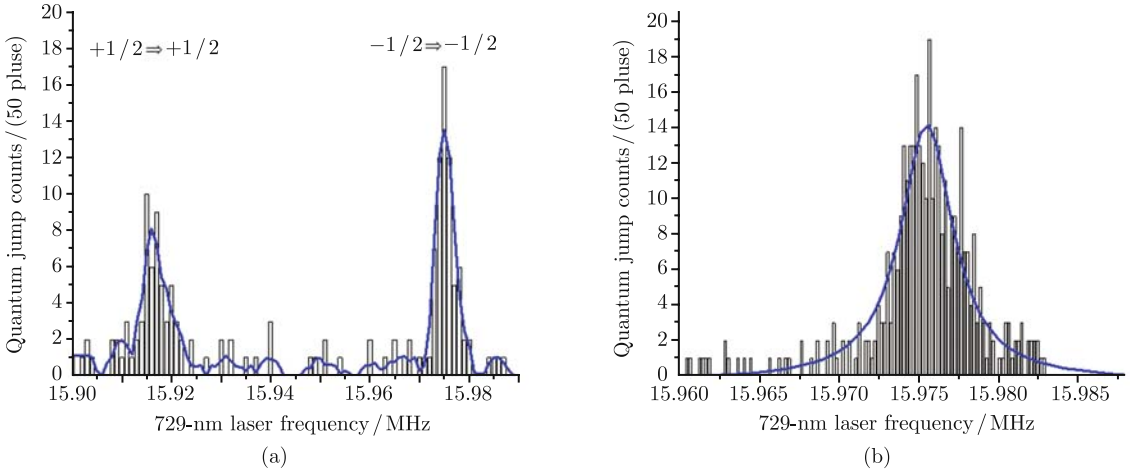

Fig. 17 **(a)** Quantum jump profile of the two $\Delta M_J = 0$ Zeeman components of the clock transition of a single $^{40}Ca^{+}$ ion. The solid profile is 5 points S–G smoothing to the bar profile. **(b)** One of the $\Delta M_J = 0$ components, which was achieved with the 729-nm scanning step of 200 Hz and 400 nW power into the trap. The magnetic field is 55 milli-Guass in the trap center. The solid profile is Lorentz curve fitting to the bar profile.

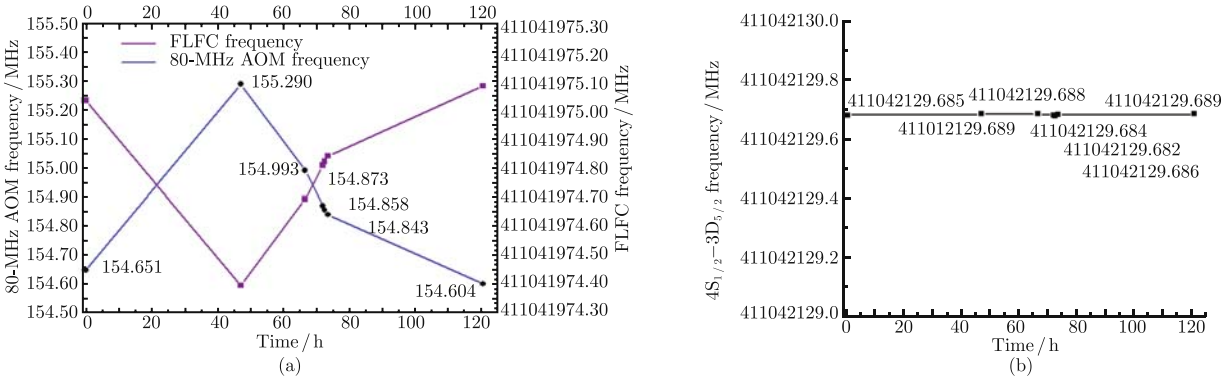

Fig. 18 **(a)** The super cavity's resonate frequency (*red line*) and the frequency detuning value (*blue line*) analyzed with quantum jump profiles using 80-MHz AOM gained during 120 hours; **(b)** Final averaged measurement result of the 729-nm electric quadrupole transition in a single $^{40}Ca^{+}$ ion.

According to the measurements made 7 times during 120 hours, the mean value of the center frequency is estimated to be 411 042 129 686.1 (2.6) kHz (Fig. 18). In these measurements, the precision of f_{AOM} is at the level of kilohertz, which can be improved by upgrading the $^{40}Ca^{+}$ ion trapping system and overcoming the systematic frequency shift.

To operate our system as a frequency standard, the attempt to lock the 729-nm laser system to atomic transition is made by the "four points locking method" [26, 27]. The lock parameters need to be optimized further.

3 Conclusions

The study of optical frequency standards has been carried out. The ion trapping system, Doppler cooling system, and fluorescence detection system are demonstrated and improved. As the breakthrough to laser stabilization techniques, laser cooling and long-time confinement of a single $^{40}Ca^{+}$ ion is achieved. Ion's laser cooling dynamics is studied in theory and experimentally to compensate for the confinement field and with the purpose of increasing signal-to-noise ratio.

With the stabilization study about the 729-nm system, the clock laser is referenced to a high-finesse ULE cavity. Preliminary frequency measurement of the electric quadrupole transition in a single laser-cooled $^{40}Ca^{+}$ ion is achieved at kilohertz level. The attempt to lock the single-ion optical frequency standard is made.

We shall develop the single-ion optical clock and evaluate its capability. Physical and environmental effects influencing the performance of the frequency standard should be studied. A magnetic field shield and new optical time sequence scheme will be tested in further experiments, with the expectation of reducing Zeeman profile's linewidth.

Acknowledgements The project was supported by the Ministry of Science and Technology of China (Grant Nos. 2005CB724500 and 2006BAK03A20), the National Natural Science Foundation of China (Grant Nos. 60490280, 10774161, 10504038, and 10874205) and the Chinese Academy of Sciences. We thank Dr. Gui-long Huang (NPL) for help and working with us, Profs. Jun Ye (JILA) and Long-sheng Ma (East China Normal University) for help and fruitful discussions; Prof. Zhi-yi Wei (IOP, CAS) and his group for the femtosecond comb system and the work together; Mr. Jin-rui Li for help with the laser system; Profs. Li-sheng Chen and Xi-wen Zhu for help and discussions; and Drs. Jiao-mei Li, Hua-lin Shu, and Hao-quan Fan for the early works.

References

1. S. A. Diddams, J. C. Bergquist, S. R. Jefferts, and C. W. Oates, Science, 2004, 306: 1318
2. H. G. Dehmelt, IEEE Trans. Instrum. Meas., 1982, 31: 83
3. R. J. Rafac, B. C. Young, J. A. Beall, W. M. Itano, D. J. Wineland, and J. C. Bergquist, Phys. Rev. Lett., 2000, 85: 2462
4. S. A. Diddams, Th. Udem, J. C. Bergquist, E. A. Curtis, R. E. Drullinger, L. Hollberg, W. M. Itano, W. D. Lee, C. W. Oates, K. R. Vogel, and D. J. Wineland, Science, 2001, 293: 825
5. P. J. Blythe, S. A. Webster, H. S. Margolis, S. N. Lea, G. Huang, S.-K. Choi, W. R. C. Rowley, P. Gill, and R. S. Windeler, Phys. Rev. A, 2003, 67: 020501
6. J. Stenger, C. Tamm, N. Haverkamp, S. Weyers, and H. R. Telle, Opt. Lett., 2001, 26: 1589
7. J. von Zanthier, Th. Becker, M. Eichenseer, A. Yu. Nevsky, Ch. Schwedes, E. Peik, H. Walther, R. Holzwarth, J. Reichert, Th. Udem, T. W. Hänsch, P. V. Pokasov, M. N. Skvortsov, and S. N. Bagayev, Opt. Lett., 2000, 25: 1729
8. H. S. Margolis, G. P. Barwood, G. Huang, H. A. Klein, S. N. Lea, K. Szymaniec and P. Gill, Science, 2004, 306: 1355
9. T. Rosenband, P. O. Schmidt, D. B. Hume, W. M. Itano, T. M. Fortier, J. E. Stalnaker, K. Kim, S. A. Diddams, J. C. J. Koelemeij, J. C. Bergquist, and D. J. Wineland, Phys. Rev. Lett., 2007, 98: 220801
10. K. Matsubara, K. Hayasaka, Y. Li, H. Ito, S. Nagano, M. Kajita, and M. Hosokawa, Appl. Phys. Express, 2008, 1: 067011
11. K. J. Siemsen, A. A. Madej, and B. G. Whitford, IEEE J. Quantum Electron., 1995, 31: 1764
12. T. Rosenband, D. B. Hume, P. O. Schmidt, C. W. Chou, A. Brusch, L. Lorini, W.H. Oskay, R. E. Drullinger, T.M. Fortier, J. E. Stalnaker, S. A. Diddams, W. C. Swann, N. R. Newbury, W. M. Itano, D. J. Wineland, and J. C. Bergquist, Science, 2008, 319: 1808
13. C. Champenois, M. Houssin, C. Lisowski, M. Knoop, M. Vedel, and F. Vedel, Phys. Lett. A, 2004, 331: 298
14. M. Kajita, Y. Li, K. Matsubara, K. Hayasaka, and M. Hosokawa, Phys. Rev. A, 2005, 72: 043404
15. F. Schmidt-Kaler, H. Häffner, M. Riebe, S. Gulde, G. P. T. Lancaster, T. Deuschle, C. Becher, C. F. Roos, J. Eschner, and R. Blatt, Nature, 2003, 422: 408
16. M. Chwalla, J. Benhelm, K. Kim, G. Kirchmair, T. Monz, M. Riebe, P. Schindler, A. S. Villar, W. Hänsel, C. F. Roos, R. Blatt, M. Abgrall, G. Santarelli, G. D. Rovera, and Ph. Laurent, Phys. Rev. Lett., 2009, 102: 023002
17. H.-L. Shu, H. Guan, X.-R. Huang, J.-M. Li, and K.-L. Gao, Chin. Phys. Lett., 2005, 22: 1641
18. H.-L. Shu, B. Guo, H. Guan, Q. Liu, X.-R. Huang, and K.-L. Gao, Chin. Phys. Lett., 2007, 24: 1217
19. H. Guan, B. Guo. G. L. Huang, H.-L. Shu, X.-R. Huang, and K.-L. Gao, Opt. Commun., 2007, 274: 182
20. B. G. Lindsay, K. A. Smith, and F. B. Dunning, Rev. Sci. Instrum., 1991, 62: 1656
21. K. Matsubara, S. Uetake, H. Ito, Y. Li, K. Hayasaka, and M. Hosokawa, Jpn. J. Appl. Phys., 2005, 44: 229
22. D. J. Berkeland, J. D. Miller, J. C. Bergquist, W. M. Itano, and D. J. Wineland, J. Appl. Phys., 1998, 83: 5025
23. V. P. Kaftandjian, C. Delsart, and J. C. Keller, Phys. Rev. A, 1981, 23: 1365
24. R. D. Cowan, The Theory of Atomic Structure and Spectra, California Univ. Press. Berkeley, 1981: 446

25. W. Zhang, Y. Y. Zhao, H. N. Han, Q, Du, Z. Y. Wei, B. Guo, Q. Liu, H. Guan, X. R. Huang, and K. L. Gao. Measurement of 729 nm optical frequency with a novel frequency comb toward $^{40}Ca^{+}$ $4s^2S_{1/2}$–$3d^2D_{5/2}$ clock transition (in preparing)
26. G. Barwood, K. Gao, P. Gill, G. Huang, and H. A. Klein, IEEE Trans. Instrum. Meas., 2001, 50: 543
27. J. E. Bernard, A. A. Madej, L. Marmet, B. G. Whitford, K. J. Siemsen, and S. Cundy, Phys. Rev. Lett., 1999, 82: 3228